

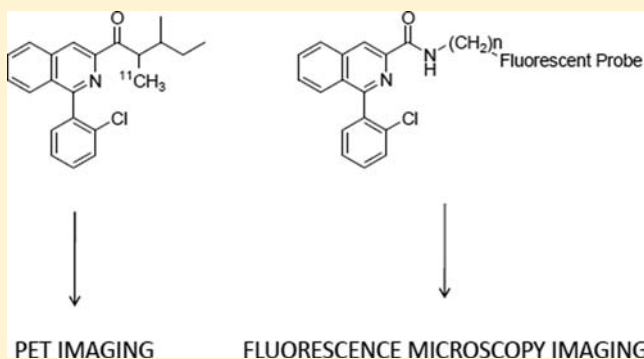
## Targeting of the Translocator Protein 18 kDa (TSPO): A Valuable Approach for Nuclear and Optical Imaging of Activated Microglia

Adriana Trapani,<sup>†</sup> Claudio Palazzo,<sup>†</sup> Modesto de Candia,<sup>†</sup> Francesco Massimo Lasorsa,<sup>‡</sup> and Giuseppe Trapani<sup>\*,†</sup>

<sup>†</sup>Department of Pharmacy and Drug Sciences, University of Bari, Bari, 70125, Italy

<sup>‡</sup>CNR Institute of Biomembranes and Bioenergetics, via Amendola, 165/a 70126, Bari, Italy

**ABSTRACT:** The aim of the present review is to give a concise and updated analysis of the imaging tools for the visualization of activated microglia. After an overview on the important pathologies where activated microglia are involved, we first describe the role played by the translocator protein-18 kDa (TSPO) as an important target for the visualization of activated microglia. Second, imaging tools based on TSPO ligands radiolabeled for positron emission tomography (PET) are summarized with particular emphasis to the TSPO ligands alternative to the standard radioligand [<sup>11</sup>C]PK11195 or (R)-[<sup>11</sup>C]PK11195. In this regard, an updated list of <sup>11</sup>C- and <sup>18</sup>F-labeled TSPO radioligands is shown. Moreover, a detailed analysis based on TSPO ligands bearing fluorescent probes for fluorescence microscopy is also provided. This last optical imaging technique represents an area of large and increasing interest due to the advantages offered by the use of simple instrumentation and safer experimental conditions. The scope and limitations of the nuclear and optical imaging techniques are discussed. Finally, a perspective on the plausible advances in this area is also presented.



### ■ INTRODUCTION

Microglia are a large population of brain cells belonging to the monocytic-macrophage cell lines. Their main function is to detect possible changes in the extracellular microenvironment of the brain that might be harmful to neurons.<sup>1,2</sup> More precisely, they are involved in immune responses against potentially cytotoxic substances, including reactive oxygen species (ROS), nitric oxide, excitatory amino acids, and cytokines. In response to a wide variety of neuronal insults in the central nervous system (CNS), microglia change from a resting phenotype to an activated phenotype. In particular, microglia that are undergoing activation show a sharp change in morphology, *i.e.*, from a ramified morphology in the resting state to an amoeboid morphology in the activated one. Once activated, microglia migrate to the site of injury where they play a phagocytic role. The primary objective of this process is to reestablish homeostasis in the brain and protect it from further impairments.<sup>3</sup>

Apart from the phagocytic and protective role, several experimental data suggest that activated microglia can release potential neurotoxins and substances influencing neuronal function as cytokines and tumor necrosis factor  $\alpha$  that may cause neuronal damage and promote neurodegeneration. The release of the proinflammatory cytokines is related to the fact that an inflammatory state occurs which may contribute to the progression of the disease. Hence, activated microglia may exert

neuroprotective effects and may be implicated in neuroinflammation processes.

Neuroinflammation is a response to different types of tissue insults leading to isolation of the damaged tissue, and it promotes immune responses. However, it is important to point out that in a recent review article Graeber et al. recommended not to use the term “neuroinflammation” and always replace it with “microglial activation” in order to avoid possible confusion about the meaning.<sup>4</sup> Microglia activation is involved in a wide range of neuropathological diseases such as Alzheimer’s (AD) and Parkinson’s disease (PD), multiple sclerosis (MS), and HIV-associated dementia, as well as in stroke and neuropsychiatric diseases.<sup>1,2,5,6</sup> Therefore, imaging of activated microglia in patients suffering from these neurological and psychiatric disorders may be useful for monitoring the inflammatory state of the CNS and for assessing the efficacy of therapeutic protocols.<sup>7,8</sup>

In the past decade, several studies showed that imaging of activated microglia in the CNS may be performed by positron emission tomography (PET) using ligands of the translocator protein 18 kDa (TSPO 18 kDa, TSPO).<sup>8,9</sup> Therefore, these TSPO ligands may be used as diagnostic tools for monitoring physiological and pathological processes in the CNS. In

**Received:** December 14, 2012

**Revised:** June 17, 2013

**Published:** July 9, 2013

Table 1. [ $^{11}\text{C}$ ]-Labeled PET Tracers for Translocator Protein 18 kDa

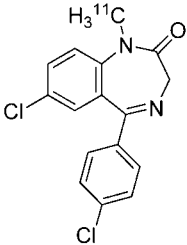
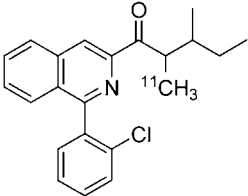
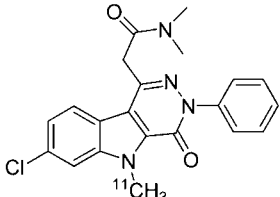
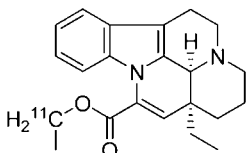
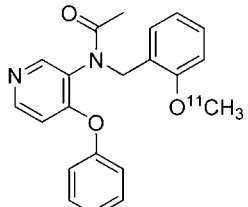
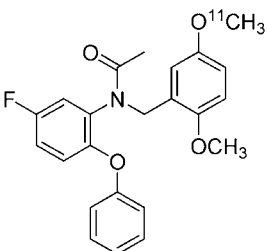
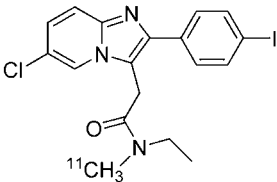
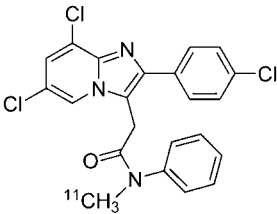
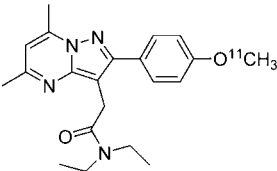
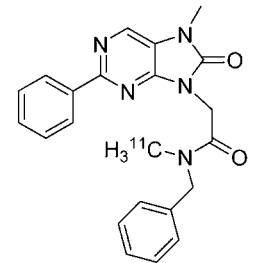
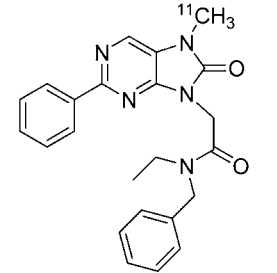
Chemical class	structure	ligand	Binding Affinity (nM) and/or Notes	Ref
Benzodiazepines		[ $^{11}\text{C}$ ]Ro 5-4864	>40 nM in humans	(36)
Quinoline carboxamides		[ $^{11}\text{C}$ ]PK 11195	2.1-28.5 nM in humans	(36)
Indoleacetamides		[ $^{11}\text{C}$ ]SSR180575	The images acquired using [ $^{11}\text{C}$ ]SSR180575 are at higher contrast than the ones obtained with [ $^{11}\text{C}$ ]PK11195. Moreover, [ $^{11}\text{C}$ ]SSR180575 has high specific binding for the TSPO.	(37)
Vinca alkaloids		[ $^{11}\text{C}$ ]Vinpocetine	A comparative study showed that [ $^{11}\text{C}$ ]vinpocetine possesses favourable characteristics over [ $^{11}\text{C}$ ]PK11195. However, further studies are necessary to propose the former ligand as microglia activation biomarker.	(38)
Phenoxyaryl-acetamides		[ $^{11}\text{C}$ ]PBR28	2.2-52 nM in humans. This radioligand possesses substantially improved signal-to-background noise ratio compared to that with [ $^{11}\text{C}$ ]PK11195. However, it was observed that there are subjects expressing the TSPO with an approximate 50-fold reduction in affinity for PBR28 (subjects low-affinity binders). Two further groups have been identified: high-affinity binders and mixed-affinity binders.	(36,23,39)
		[ $^{11}\text{C}$ ]DAA1106	< 1 nM in humans. Some studies suggest that DAA1106 might possess binding better features than those of PK11195. Moreover, in a study of patients with AD, [ $^{11}\text{C}$ ]DAA1106 yielded promising results. In fact, increased binding of TSPO in AD was showed by using	(36,23,40)

Table 1. continued

Chemical class	structure	ligand	Binding Affinity (nM) and/or Notes	Ref
Imidazopyridin- acetamides and bioisosteric structures pyrazolopyrimidines)		[ <sup>11</sup> C]CLINME	positron emission tomography with [ <sup>11</sup> C]DAA1106. However, this study did not take into account the effect of variable binding affinity typical of TSPO ligands. Therefore, although a significant increase in signal in the AD group was detected, there was a substantial overlap in the signal between low- and high-affinity binders.	(20,22,41)
		[ <sup>11</sup> C]CB148	0.203 nM in rat. Administration of [ <sup>11</sup> C]CB 148 to mice showed accumulation of radioactivity in TSPO-rich regions of the brain. Moreover, the co-injection of PK11195 reduced the accumulation of radioactivity in brain.	(42)
		[ <sup>11</sup> C]DPA-713	1.3 nM in mouse. In a comparative study between [ <sup>11</sup> C]DPA-713 and [ <sup>11</sup> C]PK11195 it has been found that in the healthy brain, the average plasma-to-tissue clearance and the volume of distribution of [ <sup>11</sup> C]DPA-713 were larger	(23,43)
Dihydro-9H- purinacetamides		[ <sup>11</sup> C]DAC	This radioligand has been found useful and sensitive biomarker for the visualization of early infarction. The TSPO expression was also found slightly increased in the infarcted brain.	(44,45)
		[ <sup>11</sup> C]AC-5216	In PET studies in mouse models of Alzheimer's disease, this radioligand showed better TSPO contrasts than [ <sup>18</sup> F]fluoroethoxy-DAA1106.	(46)

particular, specific TSPO ligands have been developed or are under development for the diagnosis of various neurological and psychiatric disorders.

The objective of this review is to discuss recent advances in imaging of activated microglia by using TSPO ligands. The main TSPO ligands for activated microglia imaging by PET will be reviewed first, and then attention will be focused to TSPO ligands used for the same purpose by optical techniques.

## ■ TRANSLOCATOR PROTEIN 18 KDA (TSPO 18 KDA, TSPO) AND ACTIVATED MICROGLIA

**TSPO: Structure and Molecular Function.** The translocator protein (18 kDa) (TSPO), previously denoted as peripheral benzodiazepine receptor (PBR), is a protein localized primarily in the outer mitochondrial membrane.<sup>10,11</sup> It is part of the mitochondrial permeability transition (MPT) pore situated at junction between the inner and the outer mitochondrial membranes.<sup>10,11</sup>

There is evidence suggesting that TSPO is a five transmembrane protein arranged to form a channel-like structure.<sup>12,13</sup> Moreover, TSPO is associated with other proteins existing in the outer and inner mitochondrial membrane, as the voltage-dependent anion channel (VDAC) and the adenine nucleotide transporter (ANT).<sup>10,11</sup> TSPO is expressed in many organs, but the highest levels occur in tissues containing steroid synthesizing cells, such as adrenal, gonad, and brain cells.<sup>10</sup> In the CNS, TSPO is expressed in microglia and in astrocytes.<sup>11</sup>

The main TSPO functions include cholesterol transport and steroid hormone synthesis, MPT pore opening, and apoptosis.<sup>14</sup>

In steroidogenic cells, TSPO mediates the translocation of cholesterol from the outer to the inner mitochondrial membrane, where it is converted by the cholesterol side-chain-cleaving cytochrome P450 enzyme (P450<sub>sc</sub>) to pregnenolone from which other neurosteroids are synthesized.<sup>11</sup> These neurosteroids are derivatives that are synthesized *de novo* from cholesterol in CNS, some of which modulate the GABA<sub>A</sub> receptor function with potencies and efficacies similar to or greater than those of benzodiazepines and barbiturates.<sup>10,11</sup>

TSPO is also implicated in the regulation of apoptotic and necrotic cell death. In fact, the MPT pore is opened by some TSPO ligands leading to an increase in the mitochondrial membrane permeability, leakage of mitochondrial pro-apoptotic factors such as caspase-3 and caspase-9, and hence induction of apoptosis and cell death.<sup>14,15</sup>

TSPO overexpression was related to microglia activation and hence considered a biomarker of neuroinflammation. It has been established that TSPO up-regulation can also occur in astrocytes. The relative distribution of microglia versus astrocyte TSPO binding is dependent on time and duration of injury.<sup>16,17</sup> It is now accepted that, at the initial stage of diseases, an increase in microglia TSPO binding occurs, then enhanced TSPO expression in astrocytes or in microglia combined with astrocytes is observed.<sup>10,11</sup> This overexpression of TSPO in activated microglia and astrocytes in diseased brain is directly related to the degree of damage. However, this time-dependent activated microglia/astrocyte colocalization makes accurate quantification and interpretation of TSPO binding by PET imaging studies difficult. Therefore, currently there is considerable interest in the search of new high-affinity and selective TSPO ligands able to overcome this limitation.

**TSPO and Imaging of Activated Microglia by PK11195.** Several studies showed that imaging of activated microglia in CNS disorders may be achieved by both nuclear [e.g., PET or single photon emission computed tomography (SPECT)] and optical [e.g., fluorescence microscopy (FM)], near-infrared fluorescence (NIRF)] imaging using appropriate TSPO ligands. Among the TSPO ligands known to date, PK-11195 (1-(2-chlorophenyl)-*N*-methyl-*N*-(1-methylpropyl)-3-isoquinoline carboxamide) (Table 1) is by far the most used ligand in animal models (including humans) with various CNS diseases.<sup>18–20</sup> Racemic PK11195 (1-(2-chlorophenyl)-*N*-methyl-*N*-(1-methylpropyl)-3-isoquinoline carboxamide) is a high-affinity and selective TSPO ligand ( $K_i = 9.3$  nM).<sup>21</sup> The *R*-enantiomer of [<sup>11</sup>C]PK11195 showed in rats a 2-fold higher affinity than the corresponding *S*-isomer, and therefore it is more useful than the racemic PK11195 or *S*-enantiomer for imaging purpose.<sup>18</sup> In the following, an overview of PET studies using racemic [<sup>11</sup>C]PK11195 or (*R*)-[<sup>11</sup>C]PK11195 in some neurological diseases is reported. For more detailed information in this regard, the reader is referred to recent excellent review articles.<sup>11,20,22,23</sup>

*In vivo* visualization of activated microglia in AD patients has been made using both racemic- and (*R*)-[<sup>11</sup>C]PK11195. In the study carried out with the racemic ligand no difference was noted between AD patients and controls.<sup>24</sup> In contrast, by using the *R*-enantiomer of PK11195 it has been shown an enhanced binding in several brain regions of AD patients as compared with healthy controls.<sup>3,25</sup> These conflicting results by PET studies further justify the interest for new specific ligands with TSPO binding affinity higher than PK11195.<sup>3</sup>

In PD patients, an increased (*R*)-[<sup>11</sup>C]PK11195 binding affinity in selected brain regions was observed, as compared with healthy controls.<sup>26</sup> Moreover, it was also noted that in the same patients the binding of (*R*)-[<sup>11</sup>C]PK11195 remained unchanged for a further two year period of observation. These results suggest that imaging of brain microglial activation using PET might be useful at early stages of disease but remains unchanged with disease progression.<sup>26</sup>

MS is a neurological disease in which the myelin sheaths around the axons of the brain and spinal cord are damaged. MS affects the ability of nerve cells in the brain and spinal cord to communicate with each other effectively. This degeneration involves the white matter of the brain and spinal cord which, indeed, is mainly composed of myelin. In post-mortem tissues of MS patients containing white matter lesions, increased TSPO expression has been found with (*R*)-[<sup>11</sup>C]PK11195 (*i.e.*, 3–4 times greater than that observed in normal white matter).<sup>27,23</sup> Besides the involvement of white matter, several studies showed a substantial implication in MS of gray matter (GM).<sup>23</sup> Thus, a large increase in [<sup>11</sup>C]PK11195 binding was also detected in cortical GM of patients with secondary progressive MS compared with healthy controls.<sup>28</sup> It has been suggested that imaging GM lesions by PET may provide important information about the disease progression. Definitely, it seems that microglial activation in MS can be visualized with PET using TSPO ligands as [<sup>11</sup>C]PK11195.

Several studies showed the presence of activated microglia in brain after stroke, and moreover, increased binding of [<sup>11</sup>C]PK11195 and (*R*)-[<sup>11</sup>C]PK11195 has been found in patients with ischemic stroke.<sup>29</sup> The increased [<sup>11</sup>C]PK11195 binding areas correspond to regions evidenced also by magnetic resonance imaging (MRI).<sup>29,30</sup> Experimental data suggest that

Table 2. [ $^{18}\text{F}$ ]-Labeled PET Tracers for Translocator Protein 18 kDa

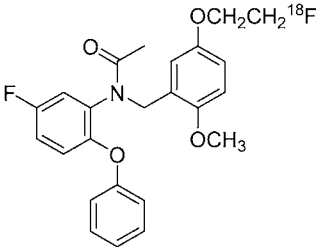
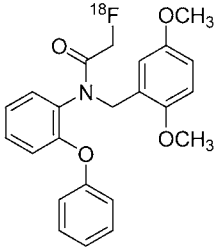
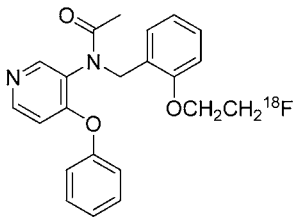
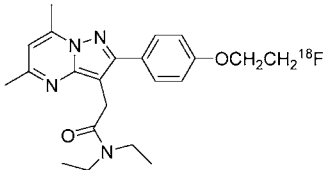
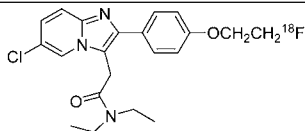
Chemical class	structure	ligand	Binding Affinity and/or Notes	Ref
Phenoxyaryl-acetamides		[ $^{18}\text{F}$ ]FEDAA1106	In patients with tau gene mutation, increased [ $^{18}\text{F}$ ]FEDAA1106 signals have been detected and the sensitivity in such cases would be enhanced including also [ $^{11}\text{C}$ ]AC-5216 as biomarker.	(46)
		[ $^{18}\text{F}$ ]PBR06	In a recent study, [ $^{18}\text{F}$ ]PBR06 and [ $^{11}\text{C}$ ]PBR28 were compared as TSPO biomarkers. It has been found that the radioligands are comparable in terms of precision and sensitivity. Thus, the choice between these radioligands should be made taking into account the notably different half-lives of the two radioisotopes $^{18}\text{F}$ and $^{11}\text{C}$ .	(47)
		[ $^{18}\text{F}$ ]-FEPPA	A recent article described the kinetic model for the binding to TSPO of this radioligand in the brain of 12 healthy volunteers. The data well fitted to a two-tissue compartment model. Estimation of the total volume of distribution in the gray matter of the brain constitutes an appropriate quantitation of TSPO with this radioligand.	(48)
Pyrazolopyrimidines		[ $^{18}\text{F}$ ]DPA-714	Two recent articles report the initial studies in humans using this radioligand. The first work shows the possibility of using [ $^{18}\text{F}$ ]DPA-714 for visualization of TSPO in patients with brain tumors.  The second paper shows that [ $^{18}\text{F}$ ]DPA-714 is a promising PET radioligand with excellent <i>in vivo</i> stability and biodistribution. Moreover, [ $^{18}\text{F}$ ]DPA-714 could constitute a sensitive tracer to measure the neuroinflammation.	(49,50)



Table 2. continued

Chemical class	structure	ligand	Binding Affinity and/or Notes	Ref
Imidazopyridin- acetamides		[ <sup>18</sup> F]PBR111	This radiotracer has been used in a rodent model of acute inflammation and compared with [ <sup>11</sup> C]CLINME, and with [ <sup>11</sup> C]PK11195. Results indicate that [ <sup>18</sup> F]PBR111 is a promising biomarker for neuroinflammation imaging. Moreover, it has been also reported a preparation of such a radiotracer according to GMP standards for application in humans.	(51,52)

PET imaging of MS with [<sup>11</sup>C]PK11195 could be used to map activated microglia in ischemic stroke.<sup>23,29</sup>

HIV-associated dementia is a neurological disorder induced by HIV infection and characterized by microglia activation. [<sup>11</sup>C]PK11195 has been used in two studies for imaging of this neurological disorder by PET.<sup>31,32</sup> However, different conclusions were obtained about the radioligand capacity to discriminate between HIV-infected patients and normal controls.<sup>31,32</sup>

The spectrum of the brain disorders showing microglial activation also includes some rare diseases such as amyotrophic lateral sclerosis (ALS) and Huntington's disease (HD). ALS is characterized by rapidly progressive weakness, muscle atrophy, spasticity, and respiratory compromise due to the degeneration of neurons located in the ventral horn of the spinal cord.<sup>33</sup> HD is a genetic brain disease leading to abnormal involuntary writhing movements and cognitive and psychiatric deficits. It is characterized by a destruction of neurons in certain brain regions.<sup>34</sup> In both cases, [<sup>11</sup>C]PK11195 has been used as a PET radioligand in imaging studies. Thus, in some brain regions of ALS patients, a significantly higher binding of radioligand compared with healthy controls was observed.<sup>22</sup> Similarly, significant increases in [<sup>11</sup>C]PK11195 binding sites have been detected in striatum and hypothalamus of HD patients compared with normal controls.<sup>34</sup>

Changes in TSPO expressions have also been detected in psychiatric disorders. Thus, activated microglia in schizophrenic patients has been studied by PET using [<sup>11</sup>C]PK11195 as radioligand. In a study carried out on seven patients a significantly higher binding of radioligand has been detected in the hippocampus than in healthy controls.<sup>35</sup>

**Limitations of [<sup>11</sup>C]PK11195 in Activated Microglia Quantification.** Although [<sup>11</sup>C] PK11195 has been used in PET studies as a marker of activated microglia for about two decades, it possesses low specific binding to TSPO. It limits the quantification of the PET findings and hence the amount of microglial activation. Thus, it is possible that [<sup>11</sup>C] PK11195 is not able to evidence low levels of activated microglia and might explain, for example, the different conclusions observed in the studies on HIV-infected patients.<sup>31,32</sup> In addition to the drawback mentioned, [<sup>11</sup>C] PK11195 shows a kinetic behavior that further limits the potential of this radioligand in quantitative analysis of microglia activation. [<sup>11</sup>C] PK11195, indeed, suffers from an extensive binding to plasma proteins whose levels change enough in neuroinflammation conditions

leading to variable kinetic results.<sup>1,20</sup> Moreover, the mentioned time-dependent relative distribution of microglia versus astrocytes TSPO binding would indicate a different biological function of microglia and astrocytes and may constitute a further difficulty in the interpretation of PET results employing a nonspecific TSPO radioligand as [<sup>11</sup>C] PK11195. Finally, it should also be taken into consideration that [<sup>11</sup>C] PK11195 shows pharmacological effects related to TSPO binding.<sup>6</sup> Besides these limitations, the short half-life of <sup>11</sup>C as radioisotope labeling [<sup>11</sup>C]-PK11195 (*i.e.*, 20.4 min) may cause notable practical difficulties in terms of distribution and use of the radiotracer batches. In this regard, <sup>18</sup>F containing radiotracers are more appropriate because of the longer half-life (*i.e.*, 109.8 min) of this radioisotope.

Altogether, these features account for the efforts by several research groups aimed at developing new PET radioligands with higher TSPO binding affinity.

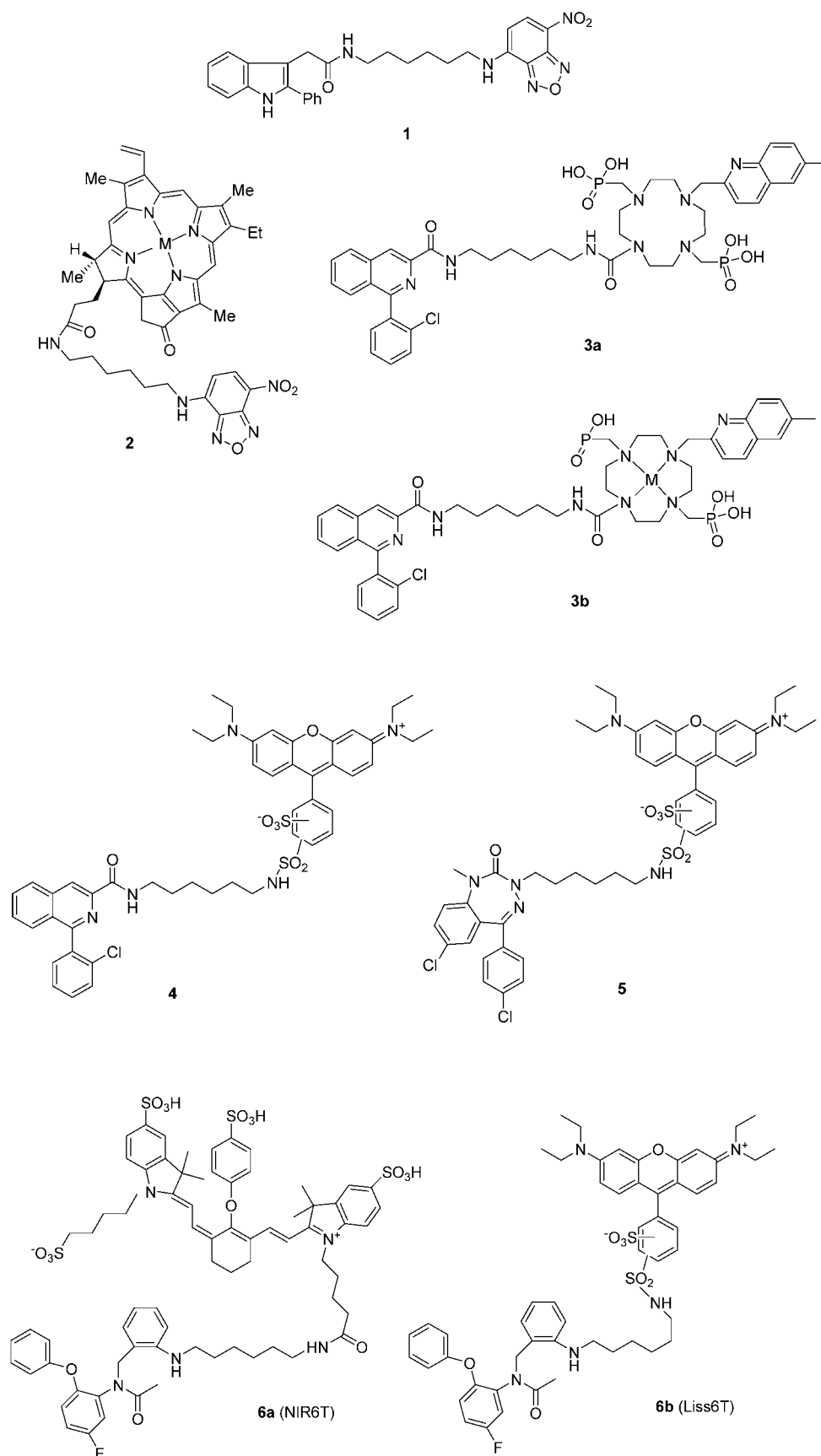
In the next section, an overview of the recent developments of TSPO radioligands for PET applications will be presented.

## ■ ACTIVATED MICROGLIA NUCLEAR VISUALIZATION BY TSPO TARGETING: THE USE OF RADIOLABELED LIGANDS DIFFERENT FROM [<sup>11</sup>C]PK11195

As an alternative to [<sup>11</sup>C]-PK11195, several specific ligands for the TSPO have been developed and used for activated microglia quantification. In Tables 1 and 2, the main <sup>11</sup>C- and <sup>18</sup>F-labeled TSPO radioligands, respectively, used for imaging of activated microglia by PET are summarized.

As can be seen, in the past years rapid development of useful new radiotracers for imaging of TSPO 18 kDa with PET has occurred. These radioligands are characterized by high affinity to the target so that a measurable signal can be generated.<sup>23</sup> Besides, to be useful from a clinical point of view, the radioligand should possess further requirements such as a quick dissociation from the target within 1–2 h that is the duration of the imaging test. To be used in imaging of brain disorders, radioligands should possess suitable lipophilicity to cross the blood brain barrier (BBB). In fact, very lipophilic radioligands lead to a high background signal due to their nonspecific binding to cell membranes.<sup>53</sup> Moreover, other complexities can arise from the metabolism of the radioligands: radiolabeled metabolites, indeed, can cross the BBB with combined signals difficult to interpret.<sup>23</sup> Finally, the synthesis of the radioligand

Chart 1. Translocator Protein 18 kDa (TSPO) Ligands Conjugated to Fluorescent Probes Developed for Activated Microglia Visualization by Fluorescence Microscopy



must be simple and rapid, in high production yield, and in agreement with GMP standards, since it must be applied in humans.<sup>52</sup>

From Tables 1 and 2, it can be deduced that new, interesting TSPO radioligands with enhanced signal-to-noise ratios are now available. However, variation in their binding affinity among subjects often make their use difficult.<sup>8,23</sup> Thus, low-affinity, high-affinity, and mixed-affinity binders are observed for the same radioligand and this makes the quantitative interpretation hard. Another aspect emerging from the examples in Tables 1 and 2 is that the main distinction between the [<sup>11</sup>C] marked radioligand and the [<sup>18</sup>F] labeled counterpart lies in the different half-lives of the isotopes with the latter being favored from a practical point of view for its longer half-life. Aside from the half-lives, there are two further factors that make the radiolabeling with <sup>18</sup>F more advantageous than that with [<sup>11</sup>C]; more specifically, (i) the synthetic labeling reactions with <sup>18</sup>F are easier and applicable to many ligands<sup>54</sup> and (ii) both the low [<sup>18</sup>F] positron energy and its short linear range in tissue (2.3 mm) lead to a better spatial resolution and give the highest resolution in PET images among all the available positron emitters.<sup>54,55</sup>

Again, it should be noted that none of these TSPO ligands contain organic functions such as amino, hydroxy, and carboxylic groups useful for further conjugation to give new diagnostic imaging agents. Finally, it is also evident that to date we still do not have PET radioligands selective for each of the two different biological functions reflected by TSPO binding (*i.e.*, microglia versus astrocyte activation).

### ■ ACTIVATED MICROGLIA OPTICAL VISUALIZATION BY TSPO TARGETING: THE USE OF LIGANDS ALTERNATIVE TO RADIOLABELED ONES

Although a number of TSPO ligands labeled with <sup>11</sup>C and <sup>18</sup>F have been developed for activated microglia visualization by PET, it is well-known that imaging studies using these radioisotopes show some drawbacks because they are limited by their short half-lives and the resolution is somewhat low. In fact, the spatial resolution attainable by PET scanners currently in clinical use is  $\geq 5$  mm, even though in recent years a new generation of PET scanners have been developed allowing improved resolution ( $\leq 5$  mm). Currently, PET-systems for small animal imaging can resolve even 1 mm, a resolution exceeded by other imaging systems as computerized tomography (CT) or magnetic resonance imaging (MRI). These new scanners, used in combination with CT or MRI, allow accurate anatomical localization of the tracer and its quantitation.<sup>56</sup> On the other hand, imaging studies based on the use of TSPO ligands labeled with <sup>3</sup>H present shortcomings because they are somewhat difficult to prepare, costly, and they generate radioactive waste.

A valuable alternative to the use of radiolabeled ligands is the activated microglia visualization by fluorescence microscopy (FM) which essentially consists of the injection of TSPO ligands conjugated to fluorescent probes in tissues and assessment of their distribution with a high resolution fluorescence microscope. This optical imaging approach enables visualization of the activated microglia, overcoming most of the drawbacks shown by PET technology. Advantages of FM imaging, indeed, comprise the requirement of simple and relatively low-cost instrumentation, the use of nonionizing radiations, and the fact that it does not produce dangerous waste and mainly allows exact localization of the injected

fluorescent probes in tissues by combining the results with *ex vivo* immunohistochemical experiments.<sup>56</sup> The main drawback of the activated microglia imaging by FM is the not elevated spatial resolution.<sup>56</sup> In fact, the spatial resolution of optical imaging techniques is restricted to about 1 mm and it is primarily due to the fact that the light becomes diffuse within the tissues for the elastic scattering of photons interacting with cellular components. This light scattering causes loss of imaging resolution and influences the penetration depth of the fluorescent radiation which is enough to reach most tissues in rodents but not in humans.<sup>57</sup> In some cases, indeed, the spatial resolution of imaging with optical methods is much lower than PET.

Another optical imaging approach for activated microglia visualization is the near-infrared fluorescence (NIRF) imaging in which the distribution *in vivo* of TSPO ligands conjugated to fluorescent probes is visualized detecting and measuring the fluorescence emitted following the illumination of the target with a light source (often laser light).<sup>56,58</sup> In this technique, optical probes with fluorescence emission in the near-infrared are used, which permits adequate in-depth penetration of tissue, and interferences from tissue autofluorescence are reduced.<sup>58</sup> Moreover, with NIRF the *in vivo* visualization of molecular targets is possible at both microscopic and macroscopic levels (*i.e.*, whole animal).<sup>58</sup> To date, the most common NIRF imaging systems used are referred to as planar methods applied in epi-illumination or trans-illumination mode.<sup>57</sup> These approaches suffer from some drawbacks mainly including the nonlinear dependence between fluorescence intensity and depth penetration.<sup>57</sup>

In this section, attention will be focused on TSPO ligands conjugated to fluorescent probes developed for activated microglia visualization by FM and NIRF.

As mentioned above, the majority of TSPO ligands studied to date does not contain organic functions such as amino, hydroxy, and carboxylic groups useful for direct conjugation with fluorescent probes. As a consequence, partial modification of the chemical structure of the TSPO ligand is required to allow the formation of a linkage with the fluorescent probe. So far, both moieties, *i.e.*, the TSPO ligand and the fluorescent probe, have been connected through a linker (spacer) which should be carefully selected because it may significantly influence the binding affinity of the resulting ligand–fluorescent probe conjugate. In fact, TSPO ligand and fluorescent probe located too closely together can reduce the affinity of the conjugate for the receptor. On the other hand, if the two moieties are located too far apart by flexible linkers, an unfavorable interaction with the target may occur due to linker bending. Another desirable requirement of the linker is that it should remain stable under normal physiological conditions to avoid the premature release of the fluorescent probe before that interaction with the target occurs.

The first example of a fluorescent probe for TSPO linked to a TSPO ligand was described by Kozikowski and co-workers.<sup>59</sup> These authors synthesized the fluorescent derivative **1** (Chart 1) in which the indoleacetamide moiety (*i.e.*, TSPO ligand FGIN-27) is linked through a hexamethylenediamine spacer to the 7-nitrobenzofurazan fluorescent (NBD) probe. The resulting conjugate showed binding affinity at nanomolar level and very close to that of PK11195 in C6–2B rat glioma cells characterized by high TSPO expression. Compound **1** has been proven to give intense fluorescent spots at cytoplasmic



level of the examined cells consistent with the mitochondrial localization of the TSPO.

Taking into account that porphyrin compounds are endogenous ligands of TSPO,<sup>10</sup> Chen et al. synthesized pyropheophorbides and their metal complexes **2** [M] In(III), Ni(II), and Zn(II)], linked through a hexamethylenediamine spacer to the NBD probe (Chart 1).<sup>60</sup> These authors showed that some complexes **2** are characterized by TSPO binding affinity at nanomolar levels and could be considered promising candidates as fluorescent probes for TSPO with strong fluorescence in the range 650–720 nm.<sup>60</sup> In particular, some indium containing complexes displayed high TSPO binding affinities.

The search for new fluorescent probes for TSPO has been significantly developed by Bornhop group who first conjugated an analogue of PK11195 to a lanthanide chelate as fluorescent probe again through a hexamethylenediamine spacer to give the fluorescent TSPO ligand **3a** (Chart 1).<sup>61,62</sup> Compound **3b**, namely, the Gd<sup>3+</sup> complex of **3a**, acts as an MRI agent. Thus, a bimodal imaging tool can be obtained, i.e., optical or MR imaging, depending on the lanthanide ion involved (Eu<sup>3+</sup> for optical or Gd<sup>3+</sup> for MR). *In vitro* experiments on C6 glioma cells showed that this “cocktail” approach is valuable for fluorescence and MR bimodal imaging.<sup>62</sup>

Next, Bornhop's research group conjugated the same PK11195 analogue with the fluorescent probe Lissamine-Rhodamine B dye once again through a hexamethylenediamine spacer leading to compound **4** denoted as Liss-ConPK11195- (Chart 1).<sup>63</sup> Binding studies on MDA-MB-231 breast cancer cells and C6 glioma cells showed that Liss-ConPK11195 specifically binds to TSPO. FM studies demonstrated the cellular uptake and distribution of Liss-ConPK11195 in TSPO overexpressing C6 glioma and MDA-MB-231 cells. In particular, fluorescence was noted at the perinuclear region and no fluorescence was detected on the cell surface, which is consistent with the mitochondrial localization of the TSPO.

Using Lissamine-Rhodamine B again as fluorescent probe and hexamethylenediamine as spacer, Bornhop's group synthesized the conjugate named C<sub>6</sub>Ro5–4864 **5** (Chart 1) where an analogue of the benzodiazepine Ro5–4864 was used as TSPO ligand.<sup>64</sup> Radioligand binding and imaging studies on MDA-MB-231 and C6 glioma cells showed that **5** is also characterized by interesting optical properties for FM imaging. However, the binding affinities of both imaging agents, **4** and **5**, were rather low (i.e., IC<sub>50</sub> 1 μM for **4** and 2.6 μM for **5**, respectively).<sup>65</sup>

In a subsequent work, the same research team conjugated an analogue of DAA1106 with IRDye 800CW, a NIR fluorescent probe, and with Lissamine-Rhodamine B through different diamine spacers (3–9 carbon linkers). The effect of the spacer length on the affinity for TSPO was evaluated and it was found that the best results in terms of both affinity and yields of production were obtained with compounds **6a** and **6b** (named NIR6T and Liss6T, respectively) characterized by a hexamethylenediamine spacer (Chart 1).<sup>65</sup> Both NIR6T and Liss6T showed binding affinities to TSPO in the nanomolar range (i.e., IC<sub>50</sub> 0.24 μM and 0.0051 μM, respectively) and were used in FM imaging studies of TSPO expressing cell lines as C6 rat glioma cells and MDA-MB-231 mammary adenocarcinoma breast cancer cells.<sup>66</sup> These cells, incubated with NIR6T and Liss6T, showed by FM studies accumulation of both agents at the mitochondrial level, while incubation with free dyes (i.e., IRDye 800CW acid and Lissamine-Rhodamine B sulfonyl

chloride) did not show significant fluorescence. From these studies, it was concluded that NIR6T and Liss6T can be considered promising agents for TSPO imaging by FM.

Although in inflammatory neurological diseases such as MS, AD, and PD the BBB is impaired, with barrier leakage and altered transporter activity,<sup>67</sup> it may be, at least in part, still functional. Hence, an evident limiting factor of the FM imaging agents **1–6** is that they should be unable to cross the BBB due to their high molecular weight (MW), high hydrogen bonding potential, and absence of specific carriers.<sup>68</sup> In contrast, for both <sup>11</sup>C and <sup>18</sup>F PET tracers listed in Tables 1 and 2, respectively, the BBB penetration by passive diffusion should not be problematic due to their MW < 500 Da and satisfactory lipophilicity estimated as calculated log P (Clog P) value.

In parallel with the Bornhop group studies, we reported our contributions to activated microglia visualization by FM. In this context, we studied a series of imidazopyridine compounds linked through different diamine spacers (2, 4, and 6 carbon linkers) to NBD fluorescent probe.<sup>69,70</sup> Among these compounds our attention was focused on the *N*-benzyl-[2-(4-chlorophenyl)-6,8-dichloroimidazo[1,2-*a*]pyridin-3-yl]-acetamide derivative linked to NBD fluorescent moiety **7** (Chart 1). This compound is characterized by a hexamethylenediamine spacer and a TSPO affinity at micromolar level (i.e., IC<sub>50</sub> value of 6.7 μM).<sup>69,70</sup> It should be noted that compound **7** was selected taking into account its log C<sub>brain</sub>/C<sub>blood</sub> (log BB) value of –0.54 estimated according to Clark's model which relates log BB to log P and polar surface area.<sup>71</sup> It is accepted that log BB values >0.3 refer to compounds which readily cross BBB, whereas log BB values <–1.0 are indicative of poorly distributed compounds in the brain.

Compound **7** was incubated with Ra2, an immortalized microglial clone, in the presence of lipopolysaccharide (LPS), an endotoxin from *Escherichia coli* and a known potent activator of microglia. FM observation showed that **7** is able to stain live Ra2 microglial cells effectively.<sup>70</sup> An *in vivo* biodistribution study carried out on compound **7** showed that, after injection in the carotid artery of adult male C57BL/6 mice and successive brain removal, it hardly penetrated into the brain.<sup>70</sup> This finding further underlines that the *in silico* estimation of physicochemical properties, as log BB values can be considered as guidelines; however, they should be treated properly. Indeed, such data can often be inaccurate and important factors as the involvement of efflux systems (e.g., P-glycoprotein) or the binding to serum proteins are not taken into account.

Again, within the series of imidazopyridineacetamide TSPO ligands, we were able to synthesize the first examples of ligands containing amino, hydroxy, and carboxylic groups useful for further conjugation and endowed with high affinity and selectivity for the Translocator protein.<sup>72</sup> Thus, we conjugated two amino-imidazopyridineacetamide ligands directly with fluorescein isothiocyanate isomer 1 (FITC) and rhodamine B isothiocyanate (RBITC) to give compounds **8–10** (Chart 1).<sup>73</sup>

Compounds **8–10** are among the most active TSPO, showing binding affinity even at subnanomolar levels (i.e., 8.34, 0.95, and 12.83 nM, respectively). Also, fluorescent compounds **8–10** were able to stain live Ra2 microglial cells efficiently as well, as it was proven that binding sites of **8** and **9** may exist on mitochondria according to the mitochondrial localization of the TSPO. After injection of compounds **8–10** in the carotid artery of adult male C57BL/6 mice and successive brain removal, it was found that these imidazopyridine compounds hardly penetrate into the brain, despite their

favorable calculated log BB values (*i.e.*,  $-0.78$ ,  $-0.62$ , and  $-0.64$  for compounds **8–10**, respectively).<sup>73</sup> Due to their poor BBB transport, compounds **8–10** were injected directly into mouse striatum and, after removal of the brain, frozen sections were prepared. Cells from the mouse striatum were stained with compounds **8–10** as shown in Figure 1.<sup>73</sup>

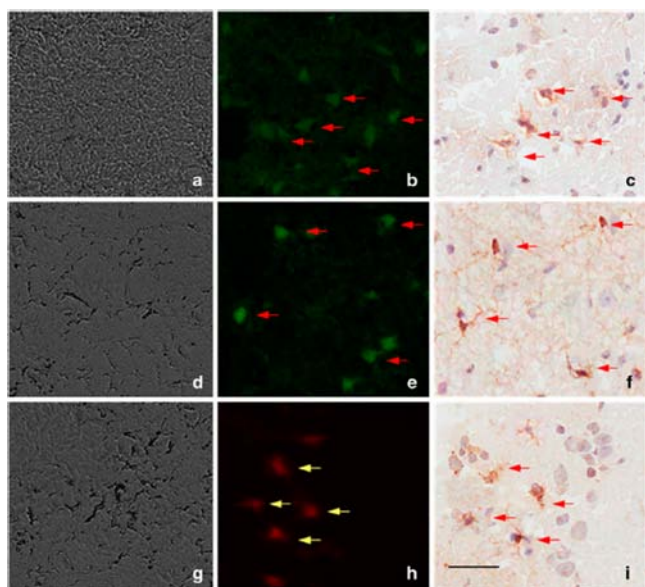


**Figure 1.** Intracranial injection indicates the compounds have reacted with CD11b-positive microglia. One of compounds **8** (a–c), **9** (d–f), and **10** (g–i) was injected into mouse striatum. Brain sections were stained with anti-CD11b antibody. (a, d, g) Phase contrast images; (b, e, h) fluorescent images; (c, f, i) CD11b staining. Arrows: double positive cells in brain sections. Scale bar: 50  $\mu\text{m}$ . (Reproduced with permission from ref 73.)

Finally, following their investigations on *N,N*-dialkyl-(2-phenylindol-3-yl)glyoxylamides as potent and selective TSPO ligands, Taliani et al. described two new fluorescent ligands for the Translocator proteins **11** and **12** (Chart 1) containing the NBD as fluorescent probe.<sup>74,75</sup> These compounds specifically and irreversibly (*i.e.*, without loss of the bound probe) labeled the TSPO at the mitochondrial level in C6 glioma cells. However, on the basis of their MW ( $>500$  Da) and log BB (*i.e.*,  $-1.04$  and  $-0.83$ , for **11** and **12**, respectively, even more negative of compounds **8–10**) values, it seems that **11** and **12** should also be endowed with limited BBB penetration features.

## CONCLUSIONS AND FUTURE PERSPECTIVES

As a result of the research undertaken over the past decade, there is nowadays general agreement that targeting TSPO constitutes a valuable approach for activated microglia visualization and thereby for diagnosis of pathophysiological processes where overexpression of the Translocator protein occurs (*e.g.*, neurological, neuropsychiatric, and tumor diseases). Consequently, activated microglia visualization can be very useful in assessing disease progression and in monitoring responses to therapeutic protocols. Among the different imaging technologies for activated microglia visualization, those based on PET are increasingly investigated. New high-affinity and -selectivity TSPO ligands able to be labeled with  $^{11}\text{C}$  and  $^{18}\text{F}$  are actively being pursued by several research groups. The goal of these efforts is the identification of PET

radioligands selective for each of the two different biological functions reflected by TSPO binding (*i.e.*, microglia versus astrocytes activation) overcoming the limitations showed by the prototype TSPO radioligand ligands (*e.g.*,  $^{11}\text{C}$ ]PK11195 and (R)- $^{11}\text{C}$ ]PK11195) used so far. However, optical imaging techniques such as those based on FM are increasingly emerging. Also, new high-affinity and -selectivity TSPO ligands conjugated with fluorescent probes are actively being pursued due to several advantages they offer, including the use of nonionizing radiation and simple instrumentation. Taken together, PET and optical imaging techniques for activated microglia visualization are very useful for this purpose. However, it is important to point out that there are marked differences in terms of scope and limitations between the two methodologies considered. First of all, as illustrated above, it is clear that the clinical relevance of the two approaches is completely different. While PET imaging is widely used in clinical practice allowing visualization of inflammation in patients with CNS disorders at high sensitivity, the optical techniques are still inadequate for *in vivo* human applications. The latter approach, indeed, is mainly applicable at preclinical levels to cell cultures and small experimental animals. Although in some work optical techniques have been used for human brain imaging, indeed, it was done either in *ex vivo* conditions after removal of the brain or during surgical procedures.<sup>56,57</sup> Instead, the binding of (R)- $^{11}\text{C}$ ]PK11195) can be currently used for the diagnosis of neurological diseases involving microglia activation in humans by PET images as illustrated in Figures 2 and 3 for AD<sup>7</sup> and PD<sup>26</sup> diseases, respectively. Concerning the optical methods, FM and NIRF imaging techniques for human brain inflammation should be regarded as highly invasive because they require even intracranial injection as shown in Figure 1 with compounds **8–10**.

It is mainly due to the fact that the penetration depth attainable by optical imaging techniques is limited by scattering of photons interacting with cellular components and it is sufficient to reach most tissues in rodents but not brain structures in humans. A further safety issue to be considered refers to the different dose required between PET and optical techniques for activated microglia imaging. Due to the high specific radioactivity of PET radioligands, only very low amounts of compound need to be administered (even at nanogram level) to obtain PET images of good quality. This implies exposure of the patient to small gamma-ray radiation, and the related risks are carefully controlled and approved. On the other hand, the dose required for imaging agents with optical techniques is greater and, hence, the toxicity associated with these fluorescent probe containing molecules may be significant. Thus, for example, in our studies on imidazopyridine **8–10**, the compounds were administered in solution with  $0.1\ \mu\text{M}$  and  $10\ \mu\text{M}$  as final concentrations for cell culture and intrarterial injection, respectively.

Finally, it should be also taken into account that, as mentioned above, the FM imaging agents currently developed (Chart 1) possess poor BBB penetration properties and it further limits their application for *in vivo* imaging of inflammation in patients with CNS disorders. Conversely, the BBB penetration should not be problematic for the radio-nuclides listed in Table 1 and Table 2, being characterized by molecular weight  $<500$  Da, low hydrogen bonding potential, and satisfactory lipophilicity. Future efforts should be directed toward the identification of fluorescent TSPO ligands of appropriate size and lipophilicity endowed with favorable BBB



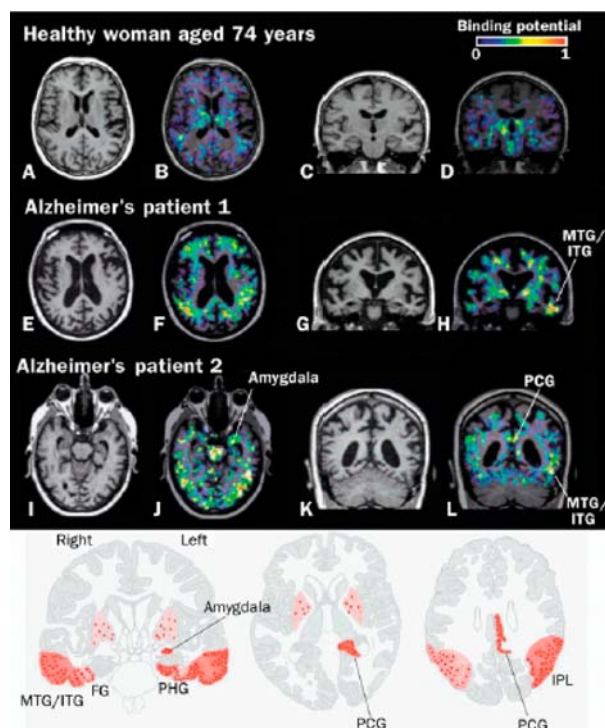


**Figure 2.** [ $^{11}\text{C}$ ](R)-PK11195 binding in healthy elderly controls and patients with Alzheimer's disease. No significant [ $^{11}\text{C}$ ](R)-PK11195 binding is seen in healthy cortex (A, C [T1-weighted MRI], B, D [MRI-PET fusion image]); however, widespread cortical [ $^{11}\text{C}$ ](R)-PK11195 binding is seen in the patient with severe dementia (E–H), with a prominent signal in the left temporal lobe (MTG/ITG = middle and inferior temporal gyrus). In the patient with moderate dementia (I–L), substantial [ $^{11}\text{C}$ ](R)-PK11195 binding is seen bilaterally in the temporal lobe but more pronounced in the left hemisphere (PCG = posterior cingulate gyrus). Schematic drawing summarizes anatomical distribution pattern of peripheral benzodiazepine binding sites (red areas) in Alzheimer's disease (FG = fusiform gyrus, PHG = parahippocampal gyrus, PCG = posterior cingulate gyrus, IPL = inferior parietal lobe). (Reproduced with permission from ref 7.)

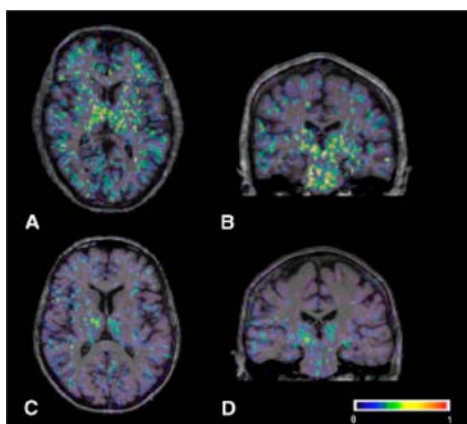


**Figure 3.** Transverse and coronal sections of binding potential maps coregistered to the individual MRI. In the PD patient (A and B), binding is increased in the basal ganglia, pons, and frontal regions, while the healthy control person (C and D) only shows constitutive [ $^{11}\text{C}$ ](R)-PK11195 binding in the thalamus and pons. The color bar denotes binding potential values from 0 to 1. (Reproduced with permission from ref 26.)

penetration properties, also making cautious use of *in silico* estimation methods.<sup>76</sup> To overcome the limitation of poor BBB penetration of the FM imaging agents, an interesting possibility might be that recently opened up by Bornhop's group who reported the first example of TSPO targeted nanocarrier delivering an optical imaging agent.<sup>77</sup> These authors linked to a fourth generation dendrimer (G(4)-PAMAM) both the PK11195 analogue previously used and the fluorescent probe Lissamine-Rhodamine B dye. *In vitro* experiments showed that this imaging agent is able to bind to the mitochondria and visualize TSPO expressing C6 rat glioma cells and MDA-MB-231 mammary breast cancer cell lines.<sup>77</sup> As pointed out by the authors, this imaging agent, acting as a nanotheranostic, i.e., a system in which disease diagnosis and therapy are combined, could allow personalized medicine and hence therapeutic treatments intended for individual patients with improved efficacy and safety.<sup>78,79</sup> These findings may open the perspective of overcoming the limited BBB transportability of the FM agents using an appropriate nanocarrier different from dendrimers whose limited effectiveness in BBB penetration is recognized.<sup>80</sup> In this context, delivery systems as polymeric nanoparticles or solid lipid nanoparticles may be more appropriate.<sup>81–83</sup>

## AUTHOR INFORMATION

### Corresponding Author

\*E-mail: giuseppe.trapani@uniba.it. Phone (039) 080-5442764. Fax (039) 080-5442724.

### Notes

The authors declare no competing financial interest.

## ACKNOWLEDGMENTS

Thanks are due to Dr. D. R. J. Owen (Division of Experimental Medicine, Imperial College, Hammersmith Hospital, London, United Kingdom) for providing us the preprint version of the paper in ref 23. The authors thank the Editorial Groups of "The Lancet", Elsevier and Springer, for the permissions to re-publish Figures 1–3.

## ABBREVIATIONS

AD, Alzheimer's disease; ALS, amyotrophic lateral sclerosis; CT, computerized tomography; FITC, fluorescein isothiocyanate isomer 1; FM, fluorescence microscopy; HD, Huntington's disease; Log BB, Log Cbrain/Cblood; LPS, lipopolysaccharide; MPT, mitochondrial permeability transition; MRI, magnetic resonance imaging; MS, multiple sclerosis; NBD, 7-nitro-benzofurazan; NIR, near-infrared fluorescence; PD, Parkinson's disease; PK11195, 1-(2-chlorophenyl)-N-methyl-N-(1-methyl-propyl)-3-isoquinoline carboxamide; PET, positron emission tomography; RBITC, Rhodamine B isothiocyanate; TSPO, translocator protein 18 kDa

## REFERENCES

- (1) Venneti, S., Lopresti, B. J., and Wiley, C. A. (2006) The peripheral benzodiazepine receptor (Translocator protein 18 kDa) in microglia: from pathology to imaging. *Prog. Neurobiol.* 80, 308–322.
- (2) Kraft, A. D., and Harry, G. J. (2011) Features of microglia and neuroinflammation relevant to environmental exposure and neurotoxicity. *Int. J. Environ. Res. Public Health* 8, 2980–3018.
- (3) Lautner, R., Mattsson, N., Scholl, M., Augutis, K., Blennow, K., Olsson, B., and Zetterberg, H. (2011) Biomarkers for microglial activation in Alzheimer's disease. *Int. J. Alzheimers Dis.*, Art. ID 939426, doi:10.4061/2011/939426

- (4) Graeber, M. B., Li, W., and Rodriguez, M. L. (2011) Role of microglia in CNS inflammation. *FEBS Lett.* 585, 3798–3805.
- (5) Perry, V. H., Nicoll, J. A., and Holmes, C. (2010) Microglia in neurodegenerative disease. *Nat. Rev. Neurol.* 6 (4), 193–201.
- (6) Chauveau, F., Boutin, H., Van Camp, N., Dollé, F., and Tavitian, B. (2008) Nuclear imaging of neuroinflammation: a comprehensive review of [ $^{11}\text{C}$ ]PK11195 challengers. *Eur. J. Nucl. Med. Mol. Imaging* 35, 2304–2319.
- (7) Cagnin, A., Brooks, D. J., Kennedy, A. M., Gunn, R. N., Myers, R., and Turkheimer, F. E. (2001) In-vivo measurement of activated microglia in dementia. *Lancet* 358, 461–467.
- (8) Seneca, N. (2011) Recent advances in positron emission tomography imaging of brain. *Drug Future* 36, 601–613.
- (9) Trapani, G., Denora, N., Trapani, A., and Laquintana, V. (2012) Recent advances in ligand targeted therapy. *J. Drug Target.* 20, 1–22.
- (10) Papadopoulos, V., Baraldi, M., Guilarte, T. R., Knudsen, T. B., Lacapere, J. J., Lindemann, P., Norenberg, M. D., Nutt, D., Weizman, A., Zhang, M. R., and Gavish, M. (2006) Translocator protein (18 kDa): new nomenclature for the peripheral-type benzodiazepine receptor based on its structure and molecular function. *Trends Pharmacol. Sci.* 27, 402–409.
- (11) Rupprecht, R., Papadopoulos, V., Rammes, G., Baghai, T. C., Fan, J., Akula, N., Groyer, G., Adams, D., and Schumacher, M. (2010) Translocator protein (18 kDa) (TSPO) as a therapeutic target for neurological and psychiatric disorders. *Nat. Rev. Drug Discovery* 9, 971–988.
- (12) Joseph-Liauzun, E., Delmas, P., Shire, D., and Ferrara, P. (1998) Topological analysis of the peripheral benzodiazepine receptor in yeast mitochondrial membranes supports a five-transmembrane structure. *J. Biol. Chem.* 273, 2146–2152.
- (13) Korkhov, V. M., Sachse, C., Short, J. M., and Tate, C. G. (2010) Three-dimensional structure of TSPO by electron cryomicroscopy of helical crystals. *Structure* 18, 677–687.
- (14) Veenman, L., Papadopoulos, V., and Gavish, M. (2007) Channel-like functions of the 18-kDa Translocator protein (TSPO): regulation of apoptosis and steroidogenesis as part of the host-defense response. *Curr. Pharm. Des.* 13, 2385–2405.
- (15) Decaudin, D., Castedo, M., Nemati, F., Beurdeley-Thomas, A., De Pinieux, G., Caron, A., Pouillart, P., Wijdenes, J., Rouillard, D., Kroemer, G., and Poupon, M.-F. (2002) Peripheral Benzodiazepine receptor ligands reverse apoptosis resistance of cancer cells in vitro and in vivo. *Cancer Res.* 62, 1388–1393.
- (16) Kuhlmann, A. C., and Guilarte, T. R. (2000) Cellular and subcellular localization of peripheral benzodiazepine receptors after trimethyltin neurotoxicity. *J. Neurochem.* 74, 1694–1704.
- (17) Maeda, J., Higuchi, M., Inaji, M., Ji, B., Haneda, E., Okauchi, T., Zhang, M. R., Suzuki, K., and Suhara, T. (2007) Phase-dependent roles of reactive microglia and astrocytes in nervous system injury as delineated by imaging of peripheral benzodiazepine receptor. *Brain Res.* 1157, 100–111.
- (18) Shah, F., Hume, S. P., Pike, V. W., Ashworth, S., and McDermott, J. (1994) Synthesis of the enantiomers of [N-methyl- $^{11}\text{C}$ ]PK 11195 and comparison of their behaviours as radioligands for PK binding sites in rats. *Nucl. Med. Biol.* 21, 573–581.
- (19) Banati, R. B. (2002) Visualising microglial activation in vivo. *Glia* 40, 206–217.
- (20) Schweitzer, P. J., Fallon, B. A., Mann, J. J., and Dileep Kumar, J. S. (2010) PET tracers for the peripheral benzodiazepine receptor and uses thereof. *Drug Discovery Today* 15, 933–942.
- (21) Cagnin, A., Gerhard, A., and Banati, R. B. (2002) In vivo imaging of neuroinflammation. *Eur. Neuropsychopharmacol.* 12, 581–586.
- (22) Doorduyn, J., deVries, E. F. J., Dierckx, R. A., and Klein, H. C. (2008) PET imaging of the peripheral benzodiazepine receptor: monitoring disease progression and therapy response in neurodegenerative disorders. *Curr. Pharm. Des.* 14, 3297–3315.
- (23) Owen, D. R. J., and Matthews, P. M. (2011) Imaging brain microglial activation using positron emission tomography and translocator protein-specific radioligands. *Int. Rev. Neurobiol.* 101, 19–39.
- (24) Groom, G. N., Junck, L., Foster, N. L., Frey, K. A., and Kuhl, D. E. (1995) PET of peripheral benzodiazepine binding sites in the microgliosis of Alzheimer's disease. *J. Nucl. Med.* 36, 2207–2210.
- (25) Edison, P., Archer, H. A., Gerhard, A., Hinz, R., Pavese, N., Turkheimer, F. E., Hammers, A., Tai, Y. F., Fox, N., Kennedy, A., Rossor, M., and Brooks, D. J. (2008) Microglia, amyloid, and cognition in Alzheimer's disease: an [ $^{11}\text{C}$ ](R) PK11195-PET and [ $^{11}\text{C}$ ]PIB-PET study. *Neurobiol. Dis.* 32, 412–419.
- (26) Gerhard, A., Pavese, N., Hotton, G., Turkheimer, F., Es, M., Hammers, A., Eggert, K., Oertel, W., Banati, R. B., and Brooks, D. J. (2006) In vivo imaging of microglial activation with [ $^{11}\text{C}$ ](R)-PK11195 PET in idiopathic Parkinson's disease. *Neurobiol. Dis.* 21, 404–412.
- (27) Banati, R. B., Newcombe, J., Gunn, R. N., Cagnin, A., Turkheimer, F., Heppner, F., Price, G., Wegner, F., Giovannoni, G., Miller, D. H., Perkin, G. D., Smith, T., Hewson, A. K., Bydder, G., Kreutzberg, G. W., Jones, T., Cuzner, M. L., and Myers, R. (2000) The peripheral benzodiazepine binding site in the brain in multiple sclerosis: quantitative in vivo imaging of microglia as a measure of disease activity. *Brain* 123, 2321–2337.
- (28) Politis, M., Giannetti, P., Su, P., Turkheimer, F., Keihaninejad, S., Wu, K., Waldman, A., Reynolds, R., Nicholas, R., and Piccini, P. (2010) Cortical microglial activation is associated with disability in secondary progressive multiple sclerosis: an in vivo imaging study. *Neurology* 74 (Suppl. 2), A290.
- (29) Thiel, A., and Heiss, W.-D. (2011) Imaging of microglia activation in stroke. *Stroke* 42, 507–512.
- (30) Gerhard, A., Schwarz, J., Myers, R., Wise, R., and Banati, R. B. (2005) Evolution of microglial activation in patients after ischemic stroke: a [ $^{11}\text{C}$ ](R)-PK11195 PET study. *Neuroimage* 24, 591–595.
- (31) Hammoud, D. A., Endres, C. J., Chander, A. R., Guilarte, T. R., Wong, D. F., Sacktor, N. C., McArthur, J. C., and Pomper, M. G. (2005) Imaging glial cell activation with [ $^{11}\text{C}$ ]-R-PK11195 in patients with AIDS. *J. Neurovirol.* 11, 346–355.
- (32) Wiley, C. A., Lopresti, B. J., Becker, J. T., Boada, F., Lopez, O. L., Mellors, J., Meltzer, C. C., Wisniewski, S. R., and Mathis, C. A. (2006) Positron emission tomography imaging of peripheral benzodiazepine receptor binding in humans immunodeficiency virus-infected subjects with and without cognitive impairment. *J. Neurovirol.* 12, 262–271.
- (33) Lasiene, J., and Yamanaka, K. (2011) Glial cells in amyotrophic lateral sclerosis. *Neurol. Res. Int.*, 718987.
- (34) Politis, M., Pavese, N., Tai, Y. F., Kiferle, L., Mason, S. L., Brooks, D. J., Tabrizi, S. J., Barker, R. A., and Piccini, P. (2011) Microglial activation in regions related to cognitive function predicts disease onset in Huntington's disease: A multimodal imaging study. *Human Brain Mapping* 32, 258–270.
- (35) Doorduyn, J., de Vries, E. F. J., Willemsen, A. T. M., de Groot, J. C., Dierckx, R. A., and Klein, H. C. (2009) Neuroinflammation in schizophrenia-related psychosis A PET study. *J. Nucl. Med.* 50, 1801–1807.
- (36) Scarf, A. M., and Kassiou, M. (2011) The Translocator Protein. *J. Nucl. Med.* 52, 677–680.
- (37) Chauveau, F., Boutin, H., Van Camp, N., Thominiaux, C., Hantraye, P., Rivron, L., Marguet, F., Castel, M. N., Rooney, T., Benavides, J., Dollé, F., and Tavitian, B. (2011) In vivo imaging of neuroinflammation in the rodent brain with [ $^{11}\text{C}$ ]SSR180575, a novel indoleacetamide radioligand of the translocator protein (18 kDa). *Eur. J. Nucl. Med. Mol. Imaging* 38, 509–514.
- (38) Gulyas, B., Toth, M., Vas, A., Shchukin, E., Kostulas, K., Hillert, J., and Halldin, C. (2012) Visualising neuroinflammation in post-stroke patients: a comparative PET study with the TSPO molecular imaging biomarkers [ $^{11}\text{C}$ ]PK11195 and [ $^{11}\text{C}$ ]vinpocetine. *Curr. Radiopharm.* 1, 19–28.
- (39) Owen, D. R., Gunn, R. N., Rabiner, E. A., Bennacef, I., Fujita, M., Kreisl, W. C., Innis, R. B., Pike, V. W., Reynolds, R., Matthews, P. M., and Parker, C. A. (2011) Mixed-affinity binding in humans with 18-kDa translocator protein ligands. *J. Nucl. Med.* 52, 24–32.



- (40) Yasuno, F., Ota, M., Kosaka, J., Ito, H., Higuchi, M., Doronbekov, T. K., Nozaki, S., Fujimura, Y., Koeda, M., Asada, T., and Suhara, T. (2008) Increased binding of peripheral benzodiazepine receptor in Alzheimer's disease measured by positron emission tomography with [ $^{11}\text{C}$ ]DAA1106. *Biol. Psychiatry* 64, 835–841.
- (41) Dollé, F., Luus, C., Reynolds, A., and Kassiou, M. (2009) Radiolabelled molecules for imaging the Translocator protein (18 kDa) using positron emission tomography. *Curr. Med. Chem.* 16, 2899–2923.
- (42) Sekimata, K., Hatano, K., Ogawa, M., Abe, J., Magata, Y., Biggio, G., Serra, M., Laquintana, V., Denora, N., Latrofa, A., Trapani, G., Liso, G., and Ito, K. (2008) Radiosynthesis and in vivo evaluation of N-[ $^{11}\text{C}$ ]methylated imidazopyridineacetamides as PET tracers for peripheral benzodiazepine receptors. *Nucl. Med. Biol.* 35, 327–334.
- (43) Endres, C. J., Pomper, M. G., James, M., Uzuner, O., Hammoud, D. A., Watkins, C. C., Reynolds, A., Hilton, J., Dannals, R. F., and Kassiou, M. (2009) Initial evaluation of  $^{11}\text{C}$ -DPA-713, a novel TSPO PET ligand in humans. *J. Nucl. Med.* 50, 1276–1282.
- (44) Yui, J., Hatori, A., Kawamura, K., Yanamoto, K., Yamasaki, T., Ogawa, M., Yoshida, Y., Kumata, K., Fujinaga, M., Nengaki, N., Fukumura, T., Suzuki, K., and Zhang, M. R. (2011) Visualization of early infarction in rat brain after ischemia using a translocator protein (18 kDa) PET ligand [ $^{11}\text{C}$ ]DAC with ultra-high specific activity. *Neuroimage* 54, 123–130.
- (45) Yui, J., Hatori, A., Yanamoto, K., Takei, M., Nengaki, N., Kumata, K., Kawamura, K., Yamasaki, T., Suzuki, K., and Zhang, M. R. (2010) Imaging of the translocator protein (18 kDa) in rat brain after ischemia using [ $^{11}\text{C}$ ]DAC with ultra-high specific activity. *Synapse* 64, 488–493.
- (46) Maeda, J., Zhang, M. R., Okauchi, T., Ji, B., Ono, M., Hattori, S., Kumata, K., Iwata, N., Saido, T. C., Trojanowski, J. Q., Lee, V. M., Staufenbiel, M., Tomiyama, T., Mori, H., Fukumura, T., Suhara, T., and Higuchi, M. (2011) In vivo positron emission tomographic imaging of glial responses to amyloid-beta and tau pathologies in mouse models of Alzheimer's disease and related disorders. *J. Neurosci.* 31, 4720–4730.
- (47) Dickstein, L. P., Zoghbi, S. S., Fujimura, Y., Imaizumi, M., Zhang, Y., Pike, V. W., Innis, R. B., and Fujita, M. (2011) Comparison of  $^{18}\text{F}$ - and  $^{11}\text{C}$ -labeled arylxyanilide analogs to measure translocator protein in humans brain using positron emission tomography. *Eur. J. Nucl. Med. Mol. Imaging* 38, 352–357.
- (48) Rusjan, P. M., Wilson, A. A., Bloomfield, P. M., Vitcu, I., Meyer, J. H., Houle, S., and Mizrahi, R. (2011) Quantitation of translocator protein binding in humans brain with the novel radioligand [ $^{18}\text{F}$ ]FEPPA and positron emission tomography. *J. Cereb. Blood Flow Metab.* 31, 1807–1816.
- (49) Tang, D., Hight, M. R., McKinley, E. T., Fu, A., Buck, J. R., Smith, R. A., Tantawy, M. N., Peterson, T. E., Colvin, D. C., Ansari, M. S., Nickels, M., and Manning, H. C. (2012) Quantitative preclinical imaging of TSPO expression in glioma using N,N-diethyl-2-(2-(4-(2- $^{18}\text{F}$ -fluoroethoxy)phenyl)-5,7-dimethylpyrazolo[1,5-a]pyrimidin-3-yl)acetamide. *J. Nucl. Med.* 53, 287–294.
- (50) Arlicot, N., Vercouillie, J., Ribeiro, M. J., Tauber, C., Venel, Y., Baulieu, J. L., Maia, S., Corcia, P., Stabin, M. G., Reynolds, A., Kassiou, M., and Guilleaume, D. (2012) Initial evaluation in healthy humans of [ $^{18}\text{F}$ ]DPA-714, a potential PET biomarker for neuroinflammation. *Nucl. Med. Biol.* 39, 570–578.
- (51) Van, C. N., Boisgard, R., Kuhnast, B., Theze, B., Viel, T., Gregoire, M. C., Chauveau, F., Boutin, H., Katsifis, A., Dollé, F., and Tavitian, B. (2010) In vivo imaging of neuroinflammation: a comparative study between [(18F)]PBR111, [(11C)]CLINME and [(11C)]PK11195 in an acute rodent model. *Eur. J. Nucl. Med. Mol. Imaging* 37, 962–972.
- (52) Kuhnast, B., Damont, A., Hinnen, F., Catarina, T., Demphel, S., Le Helleix, S., Coulon, C., Goutal, S., Gervais, P., and Dollé, F. (2012) [ $^{18}\text{F}$ ]DPA-714, [ $^{18}\text{F}$ ]PBR111 and [ $^{18}\text{F}$ ]FEDAA1106—Selective radioligands for imaging TSPO 18 kDa with PET: Automated radiosynthesis on a TRACERLab FX-FN synthesizer and quality controls. *Appl. Radiat. Isot.* 70, 489–497.
- (53) Guo, Q., Brady, M., and Gunn, R. N. (2009) A biomathematical modeling approach to central nervous system radioligand discovery and development. *J. Nucl. Med.* 50, 1715–1723.
- (54) Miller, P. W., Long, N. J., Vilar, R., and Gee, A. D. (2008) Synthesis of  $^{11}\text{C}$ ,  $^{18}\text{F}$ ,  $^{15}\text{O}$ , and  $^{13}\text{N}$  radiolabels for Positron Emission Tomography. *Angew. Chem., Int. Ed.* 47, 8998–9033.
- (55) Levin, C. S., and Hoffman, E. J. (1999) Calculation of positron range and its effect on the fundamental limit of positron emission tomography system spatial resolution. *Phys. Med. Biol.* 44, 781–799.
- (56) Wunder, A., Klohs, J., and Dirnagl, U. (2009) Non-invasive visualization of CNS inflammation with nuclear and optical imaging. *Neuroscience* 158, 1161–1173.
- (57) Ntziachristos, V. (2006) Fluorescence molecular imaging. *Annu. Rev. Biomed. Eng.* 8, 1–33.
- (58) Hilderbrand, S. A., and Weissleder, R. (2010) Near-infrared fluorescence: application to in vivo molecular imaging. *Curr. Opin. Chem. Biol.* 14, 71–79.
- (59) Kozikowski, A. P., Kotoula, M., Ma, D., Boujrad, N., Tuckmantel, W., and Papadopoulos, V. (1997) Synthesis and biology of a 7-nitro-2,1,3-benzoxadiazol-4-yl derivative of 2-phenylindole-3-acetamide: a fluorescent probe for the peripheral-type benzodiazepine receptor. *J. Med. Chem.* 40, 2435–2439.
- (60) Chen, Y., Zheng, X., Dobhal, M. P., Gryshuk, A., Morgan, J., Dougherty, T. J., Oseroff, A., and Pandey, R. K. (2005) Methyl pyrophorbide-R analogues: potential fluorescent probes for the peripheral-type benzodiazepine receptor. Effect of central metal in photosensitizing efficacy. *J. Med. Chem.* 48, 3692–3695.
- (61) Manning, H. C., Goebel, T., Marx, J. N., and Bornhop, D. J. (2002) Facile efficient conjugation of a trifunctional lanthanide chelate to a peripheral benzodiazepine receptor ligand. *Org. Lett.* 4, 1075–1078.
- (62) Manning, H. C., Goebel, T., Thompson, R. C., Price, R. R., Lee, H., and Bornhop, D. J. (2004) Targeted molecular imaging agents for cellular-scale bimodal imaging. *Bioconjugate Chem.* 15, 1488–1495.
- (63) Manning, H. C., Smith, S. M., Sexton, M., Haviland, S., Bai, M., Cederquist, K., Stella, N., and Bornhop, D. J. (2006) A peripheral benzodiazepine receptor targeted agent for in vitro imaging and screening. *Bioconjugate Chem.* 17, 735–740.
- (64) Bai, M., Wyatt, S., Han, Z., Papadopoulos, V., and Bornhop, D. J. (2007) A novel conjugable translocator protein ligand with a fluorescent dye for in vitro imaging. *Bioconjugate Chem.* 18, 1118–1122.
- (65) Bai, M., Rone, M. B., Papadopoulos, V., and Bornhop, D. J. (2007) A novel functional translocator protein ligand for cancer imaging. *Bioconjugate Chem.* 18, 2018–2023.
- (66) Wyatt, S. K., Manning, H. C., Bai, M., Bailey, S. N., Gallant, P., Ma, G., McIntosh, L., and Bornhop, D. J. (2010) Molecular imaging of the Translocator Protein (TSPO) in a pre-clinical model of breast cancer. *Mol. Imaging Biol.* 12, 349–358.
- (67) Deo, A. K., Theil, F. P., and Nicolas, J. M. (2013) Confounding parameters in preclinical assessment of Blood-Brain Barrier permeation: an overview with emphasis on species differences and effect of disease states. *Mol. Pharmaceutics* 10, 1581–1595.
- (68) Denora, N., Trapani, A., Laquintana, V., Lopodota, A., and Trapani, G. (2009) Recent advances in medicinal chemistry- and pharmaceutical technology-strategies for drug delivery to the brain. *Curr. Top. Med. Chem.* 9, 182–196.
- (69) Trapani, G., Laquintana, V., Denora, N., Trapani, A., Lopodota, A., Latrofa, A., Franco, M., Serra, M., Pisu, M. G., Floris, I., Sanna, E., Biggio, G., and Liso, G. (2005) Structure–activity relationships and effects on neuroactive steroid synthesis in a series of 2-phenylimidazo-[1,2-a]pyridineacetamide peripheral benzodiazepine receptors ligands. *J. Med. Chem.* 48, 292–305.
- (70) Laquintana, V., Denora, N., Lopodota, A., Suzuki, H., Sawada, M., Serra, M., Biggio, G., Latrofa, A., Trapani, G., and Liso, G. (2007) N-Benzyl-2-(6,8-dichloro-2-(4-chlorophenyl)imidazo[1,2-a]pyridin-3-yl)-N-(6-(7-nitrobenzo[c][1,2,5]oxadiazol-4-ylamino)hexyl)-acetamide as a new fluorescent probe for peripheral benzodiazepine



receptor and microglial cell visualization. *Bioconjugate Chem.* 18, 1397–1407.

(71) Clark, D. E. (1999) Rapid calculation of polar molecular surface area and its application to the prediction of transport phenomena. 2. Prediction of blood-brain barrier penetration. *J. Pharm. Sci.* 88, 815–821.

(72) Denora, N., Laquintana, V., Pisu, M. G., Dore, R., Murru, L., Latrofa, A., Trapani, G., and Sanna, E. (2008) 2-Phenyl-imidazo[1,2-a]pyridine compounds containing hydrophilic groups as potent and selective ligands for peripheral benzodiazepine receptors: synthesis, binding affinity and electrophysiological studies. *J. Med. Chem.* 51, 6876–88.

(73) Denora, N., Laquintana, N., Trapani, A., Suzuki, H., Sawada, M., and Trapani, G. (2011) New fluorescent probes targeting the mitochondrial-located translocator protein 18 kDa (TSPO) as activated microglia imaging agents. *Pharm. Res.* 28, 2820–2832.

(74) Taliani, S., Simorini, F., Sergianni, V., La Motta, C., Da Settimo, F., Cosimelli, B., Abignente, E., Greco, G., Novellino, E., Rossi, L., Gremigni, V., Spinetti, F., Chelli, B., and Martini, C. (2007) New fluorescent 2-phenylindolglyoxylamide derivatives as probes targeting the peripheral-type benzodiazepine receptor: design, synthesis, and biological evaluation. *J. Med. Chem.* 50, 404–407.

(75) Taliani, S., Da Pozzo, E., Bellandi, M., Bendinelli, S., Pugliesi, I., Simorini, F., La Motta, C., Salerno, S., Marini, A. M., Da Settimo, F., Cosimelli, B., Greco, G., Novellino, E., and Martini, C. (2010) Novel irreversible fluorescent probes targeting the 18 kDa translocator protein: synthesis and biological characterization. *J. Med. Chem.* 53, 4085–4093.

(76) Mensch, J., Oyarzabal, J., Mackie, C., and Augustijns, P. (2009) *In vivo*, *in vitro* and *in silico* methods for small molecule transfer across the BBB. *J. Pharm. Sci.* 98, 4429–4468.

(77) Samuelson, L. E., Dukes, M. J., Hunt, C. R., Casey, J. D., and Bornhop, D. J. (2009) TSPO targeted dendrimer imaging agent: synthesis, characterization and cellular internalization. *Bioconjugate Chem.* 20, 2082–2089.

(78) Lammers, T., Kiessling, F., Hennink, W. E., and Storm, G. (2010) Nanotheranostics and image-guided drug delivery: current concepts and future directions. *Mol. Pharmaceutics* 7, 1899–1912.

(79) Bhojani, M. S., Van Dort, M., Rehemtulla, A., and Ross, B. D. (2010) Targeted imaging and therapy of brain cancer using theranostic nanoparticles. *Mol. Pharmaceutics* 7, 1921–1929.

(80) Perez-Martinez, F. C., Ocaña, A. V., Perez-Carrion, M. D., and Ceña, V. (2012) Dendrimers as vectors for genetic material delivery to the Nervous System. *Curr. Med. Chem.* 19, 5101–5108.

(81) Tosi, G., Costantino, L., Ruozzi, B., Forni, F., and Vandelli, M. A. (2008) Polymeric nanoparticles for the drug delivery to the central nervous system. *Expert Opin. Drug Delivery* 5, 155–174.

(82) Mistry, A., Stolnik, S., and Illum, L. (2009) Nanoparticles for direct nose-to-brain delivery of drugs. *Int. J. Pharm.* 379, 146–157.

(83) Blasi, P., Giovagnoli, S., Schoubben, A., Ricci, M., and Rossi, C. (2007) Solid lipid nanoparticles for targeted brain drug delivery. *Adv. Drug Delivery Rev.* 59, 454–477.